

Multi-market Participation of a Renewable Power-to-Hydrogen Facility with Battery Storage

Nikolina Čović

University of Zagreb

Faculty of Electrical

Engineering and Computing

Zagreb, Croatia

Email: nikolina.covic@fer.hr

Ivan Pavić

University of Zagreb

Faculty of Electrical

Engineering and Computing

Zagreb, Croatia

Email: ivan.pavic@fer.hr

Hrvoje Pandžić

University of Zagreb

Faculty of Electrical

Engineering and Computing

Zagreb, Croatia

Email: hrvoje.pandzic@fer.hr

Ivan Andročec

Croatian Power

Utility – HEP d.d.

Zagreb, Croatia

Email: ivan.androcec@hep.hr

Abstract—According to the European Union strategies, efforts must be undertaken to replace fossil-fueled technologies with low-carbon and renewable ones by 2050. Alongside renewable energy sources, hydrogen gradually takes the lead in decarbonizing the energy sector. The paper presents an optimization model of a low-carbon power plant consisting of a battery storage, an electrolyzer and a PV plant, participating in the day-ahead electricity and gas markets. Additionally, the plant also takes part in reserve and balancing electricity markets. The influence of different sizes of battery storage and electrolyzer on the proposed system is evaluated, together with the impact of changes in market prices.

Index Terms—battery energy storage, electrolyzer, PV, gas market, balancing markets

I. INTRODUCTION

A. Motivation

The 2015 Paris Agreement seeks to halt the average temperature rise above 2°C and keep it below 1.5°C [1]. As a result, the European Union has set itself a goal of becoming the first climate-neutral continent by 2050. To achieve this, it is necessary to reduce greenhouse gas emissions by 55% by 2030. The energy sector, as the second-largest source of greenhouse gas emissions (25%) in 2019, represents an exceptional potential for achieving this [2]. It is necessary to reduce the use of fossil fuels and increase the share of renewable energy sources. According to [3], in 2021, 22% of the EU's energy consumption came from gaseous fuels, of which 95% were fossil fuels. With the implementation of green strategies, it is expected that in 2050 the share of consumption of gaseous fuels in the EU will be around 20% and 2/3 of that will be low-carbon and renewable gases, an example of which is hydrogen. European strategies aim to have a production of 1 million tonnes of hydrogen per year by 2024, and by 2030 this amount should increase to 10 million tonnes per year.

As a part of the energy sector, hydrogen can be used to foster the decarbonization of both the power and the gas systems. Electrolyzers coupled with renewable sources can use surplus renewable electricity, convert it into renewable or green hydrogen, and feed it into a hydrogen system. For

now, there are no uniform rules on how hydrogen systems should work. For example, the ownership relations of the infrastructure required for the transfer and use of hydrogen are not defined, just as the quality level of the produced hydrogen. All of this prevents the creation of a hydrogen market and the required infrastructure [3]. However, some efforts are already in place to either mix hydrogen with natural gas or to use the existing gas infrastructure as a new hydrogen backbone and eventually a hydrogen market. A project in Denmark demonstrates that hydrogen can be injected to make up to 15% of the mixture in the gas grid without an additional leakage [4]. Another study in the Netherlands proposes the development of a dedicated hydrogen grid from the existing gas pipelines [5] and a dedicated hydrogen exchange using the current gas/electricity markets as role models [6]. Hydrogen is positioning itself as a fuel of the future, which is why analyses of the impact of its production on the energy system are needed.

The main technology to balance renewable power generation in the last couple of years has been battery energy storage [7]. Apart from the local power plant balancing, it can provide other services (e.g. balancing services [8] or grid services [9]) to create multiple sources of income. It is, therefore, of great importance to study what are the mutual interdependencies of a battery energy storage and an electrolyzer within a renewable power plant.

B. Literature Review

Hydrogen, as part of the green electricity transition, is interesting for providing ancillary services to the system. The authors in [10] analyze whether electrolyzers can provide these services. It turns out electrolyzers can be used to avoid the deviations caused by the variability of renewable energy sources. In [11], a power-to-gas plant is modeled in which an electrolyzer must provide the necessary amounts of hydrogen for the charging station, while at the same time providing auxiliary services to the power system. Although electrolyzers can provide reserve services, compared to batteries [12] and supercapacitors [13] they react too slowly to sudden and rapid changes.

A number of papers analyze the possibility of injecting hydrogen into the gas network and the impacts of doing it. In

[14] the authors consider which pipelines need to be replaced and whether to invest in new equipment, such as compressors. The effect of hydrogen injection on the gas system and the composition of the gas mixture is observed in [15]. Although there are regulations that limit the hydrogen concentration in the gas network, some processes, such as methanation in [16] allow easier and greater injection of hydrogen into the network.

Green hydrogen is produced by using (excess) renewable energy sources power production to operate an electrolyzer. In [17], the authors observe hydrogen production from alkaline electrolyzers considering variations in temperature, electrolyte weight concentration and electrode-diaphragm distance. The production by using PEM electrolyzers and energy from PV was analyzed in [18]. Increasing solar irradiance leads to higher hydrogen production, together with higher electrolysis efficiencies. The authors in [19] present a model of a PV-electrolyzer system to achieve maximum hydrogen production, with the least possible losses of power production from PV. The model in [20] is similar to the previous one, but with the wind farm as a renewable energy source. Papers [21]–[25] deal with determining the optimal size of an electrolyzer and other available units to meet the consumption, reduce costs or reduce the curtailment of energy from renewable sources in various weather conditions and consumption scenarios.

C. Contribution

This paper studies the operation of a system consisting of an electrolyzer and battery energy storage coupled with a PV power plant. Unlike the published papers, this paper presents a model of a low-carbon power plant's participation in both, electricity and gas, energy and electricity reserve markets. Participation in the electricity energy market is enabled through the purchase of electricity needed for the operation of the electrolyzer or charging the battery storage, as well as through the sale of electricity from the battery storage and the PV, shown in Fig. 1 with blue arrows. The battery storage, except in the mentioned market, can participate in the automatic frequency restoration reserve (aFRR) market by offering a certain capacity and balancing energy (dashed orange arrows in Fig. 1). The electrolyzer can provide aFRR to the power system as well, by reducing or increasing its hydrogen production (dashed orange arrows in Fig. 1). Besides, the green hydrogen produced by the electrolyzer can be injected into the gas network, which enables the sale of hydrogen in the gas market.

D. Paper Structure

Mathematical model of the facility operation is given in Section II, while the case study is presented in Section III, including the input data and the results of analyses conducted for different sizes of the electrolyzer, the battery storage and the PV plant, as well as for different market prices. Finally, Section IV concludes the paper.

II. MATHEMATICAL MODEL

Objective function (1) of the previously described facility maximizes its profit that can be generated by the day-ahead

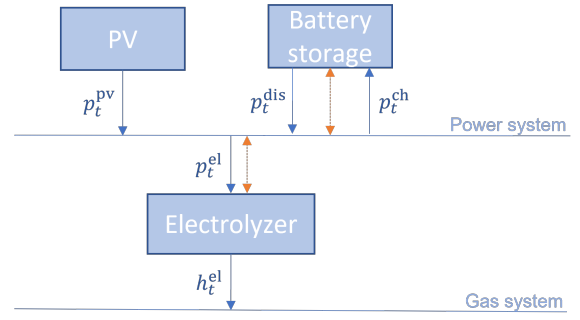


Fig. 1: A scheme of facility units' connection to gas and power system

market trading and the reserve market trading, while also considering the electricity grid charges over a set of variables $\Pi = \{p_t^{\text{dis}}, p_t^{\text{ch}}, p_t^{\text{pv}}, p_t^{\text{el}}, p_t^{\text{r,ch}}, p_t^{\text{i,dis}}, p_t^{\text{r,el}}, p_t^{\text{r,dis}}, p_t^{\text{i,ch}}, p_t^{\text{i,el}}\}$. The first line in (1) defines the profit realized in the electricity day-ahead market by trading the amount p_t^{da} at price $\lambda_t^{\text{da,p}}$ and the income realized in the gas market by selling hydrogen h_t^{el} produced by the electrolyzer at price $\lambda_t^{\text{da,g}}$. Revenue generated by the reservation of capacity for aFRR up (r_t^{u}) and down (r_t^{d}) provision at the corresponding prices ($\lambda_t^{\text{u,bc}}, \lambda_t^{\text{d,bc}}$) is formulated in the second line of the objective function. It is assumed that a certain part of the reserved capacity ($A^{\text{u}}, A^{\text{d}}$) is activated for the purpose of balancing the system. Profit from the balancing energy is given in the third line of (1). The last line corresponds to the cost of paying the grid fees. In addition to paying grid fees for purchased energy p_t^{w} at price $\lambda_t^{\text{w,p}}$, which is the first sum, it is necessary to pay grid fees for the maximum monthly withdrawn (p_m^{wm}) and injected (p_m^{inm}) power (the second sum), as well.

$$\begin{aligned} \max_{\Pi} \quad & \sum_t p_t^{\text{da}} \cdot \Delta t \cdot \lambda_t^{\text{da,p}} + \sum_t h_t^{\text{el}} \cdot \Delta t \cdot \lambda_t^{\text{da,g}} \\ & + \sum_t r_t^{\text{u}} \cdot \lambda_t^{\text{u,bc}} + \sum_t r_t^{\text{d}} \cdot \lambda_t^{\text{d,bc}} \\ & + \sum_t A^{\text{u}} \cdot \Delta t \cdot r_t^{\text{u}} \cdot \lambda_t^{\text{u,be}} - \sum_t A^{\text{d}} \cdot \Delta t \cdot r_t^{\text{d}} \cdot \lambda_t^{\text{d,be}} \\ & - \sum_t (p_t^{\text{w}} \cdot \Delta t \cdot \lambda_t^{\text{w,p}}) - \sum_m (p_m^{\text{wm}} \cdot \lambda_m^{\text{wm}} + p_m^{\text{inm}} \cdot \lambda_m^{\text{inm}}) \quad (1) \end{aligned}$$

Constraint (2) limits the production from PV (p_t^{pv}). In case the market price is unfavorable, it is possible to reject a part of the PV production.

$$p_t^{\text{pv}} \leq P_t^{\text{pv}}, \quad \forall t \quad (2)$$

Energy needed to charge the battery p_t^{ch} is purchased in the day-ahead market, as well as the energy needed to operate the electrolyzer p_t^{el} . On the other hand, it is possible to sell the energy discharged from the battery p_t^{dis} , along with the energy produced from the PV. Thus, equation (3) is a power balance constraint.

$$p_t^{\text{da}} = p_t^{\text{dis}} - p_t^{\text{ch}} + p_t^{\text{pv}} - p_t^{\text{el}}, \quad \forall t \quad (3)$$

The capacity that can be reserved for system balancing can come either from the battery storage or the electrolyzer,

as given in (4) and (5). The battery storage can provide upward reserve r_t^u by reducing the charging $p_t^{r, \text{ch}}$ and/or by increasing the discharging $p_t^{i, \text{dis}}$, while the electrolyzer can provide upward reserve by reducing the production of hydrogen, i.e. by reducing the electricity consumption $p_t^{r, \text{el}}$. In case of the downward reserve, the battery storage can reduce discharging ($p_t^{r, \text{dis}}$) and/or increase charging ($p_t^{i, \text{ch}}$), while the electrolyzer can increase its electricity consumption ($p_t^{i, \text{el}}$) and, consequently, the hydrogen production.

$$r_t^u = p_t^{r, \text{ch}} + p_t^{i, \text{dis}} + p_t^{r, \text{el}}, \quad \forall t \quad (4)$$

$$r_t^d = p_t^{r, \text{dis}} + p_t^{i, \text{ch}} + p_t^{i, \text{el}}, \quad \forall t \quad (5)$$

Equations (6)–(8) are power balance constraints that include reserve activations. Constraint (6) ensures sufficient power in case the average assumed energy for providing reserves is activated. However, even in extreme cases, when full capacity is activated in either upward or downward direction, the power balance must be maintained, which is ensured through equations (7) and (8).

$$p_t^{\text{da}} + A^u \cdot r_t^u - A^d \cdot r_t^d = p_t^{\text{in}} - p_t^{\text{w}}, \quad \forall t \quad (6)$$

$$p_t^{\text{da}} + r_t^u = p_t^{\text{u, in}} - p_t^{\text{u, w}}, \quad \forall t \quad (7)$$

$$p_t^{\text{da}} - r_t^d = p_t^{\text{d, in}} - p_t^{\text{d, w}}, \quad \forall t \quad (8)$$

At time period t it is possible to either inject energy into the network or to withdraw it, as modeled by constraints (9) and (10). Simultaneous injection and withdrawal are disabled by the binary variable $x^{i, \text{P}}$, where superscript i ensures the validity of the constraint for the average and both worst cases – upward and downward. In addition, the power that can be withdrawn is limited by P^{w} , and the power that is injected cannot exceed P^{in} .

$$p_t^{i, \text{w}} \leq P^{\text{w}} \cdot (1 - x^{i, \text{P}}), \quad \forall t, i \in \{\emptyset, u, d\} \quad (9)$$

$$p_t^{i, \text{in}} \leq P^{\text{in}} \cdot x^{i, \text{P}}, \quad \forall t, i \in \{\emptyset, u, d\} \quad (10)$$

Constraints (11) and (12) determine the maximum monthly power withdrawn or injected to the grid, respectively.

$$p_t^{\text{w}} \leq p_m^{\text{wm}}, \quad \forall m, t \quad (11)$$

$$p_t^{\text{in}} \leq p_m^{\text{inm}}, \quad \forall m, t \quad (12)$$

Constraints (13)–(20) represent limits on the charging and discharging power of battery storage. The charging and discharging power must not exceed the installed capacity of the storage P^{b} , which is modeled in (13) and (14). Besides, the charging and discharging process cannot occur concurrently, which is disabled with binary variable x_t^{b} .

$$p_t^{\text{ch}} \leq x_t^{\text{b}} \cdot P^{\text{b}}, \quad \forall t \quad (13)$$

$$p_t^{\text{dis}} \leq (1 - x_t^{\text{b}}) \cdot P^{\text{b}}, \quad \forall t \quad (14)$$

In constraint (15) the battery storage can reduce its charging power at time period t by amount p_t^{ch} , at which is charged at that time. Also, the resulting charging power after the reduction must meet the condition that the charging power must not exceed the installed battery power, which is modeled in (16). The battery storage can provide upward reserve also by increasing the discharging at time period t . However, it

must not exceed the installed power of the battery storage, as indicated in constraint (17). Namely, in case of the battery storage already charging at time period t , it can provide upward reserve by both reducing the charging power and increasing the discharging power. For that matter, the charging needs to be completely stopped first, and then the discharge power can be increased following (17). The described case is mathematically modeled using binary variable $x_t^{\text{u, b}}$. Constraints (18)–(20) describe the same process for the downward reserve.

$$p_t^{r, \text{ch}} \leq p_t^{\text{ch}}, \quad \forall t \quad (15)$$

$$p_t^{\text{ch}} - p_t^{r, \text{ch}} \leq x_t^{\text{u, b}} \cdot P^{\text{b}}, \quad \forall t \quad (16)$$

$$p_t^{i, \text{dis}} \leq (1 - x_t^{\text{u, b}}) \cdot P^{\text{b}} - p_t^{\text{dis}}, \quad \forall t \quad (17)$$

$$p_t^{r, \text{dis}} \leq p_t^{\text{dis}}, \quad \forall t \quad (18)$$

$$p_t^{i, \text{ch}} \leq (1 - x_t^{\text{d, b}}) \cdot P^{\text{b}} - p_t^{\text{ch}}, \quad \forall t \quad (19)$$

$$p_t^{\text{dis}} - p_t^{r, \text{dis}} \leq x_t^{\text{d, b}} \cdot P^{\text{b}}, \quad \forall t \quad (20)$$

Furthermore, constraints (21)–(24) limit and define state-of-energy of the battery storage at any time period t . The state of energy (soe_t) cannot exceed the installed capacity (SOE^{b}), as modeled in (21). Given the possibility of providing the balancing services, the battery storage must at all times have a guaranteed state of energy within the limits in case of activation of the entire reserved capacity. Thus, in case of activation of the entire downward capacity, the battery storage cannot be charged above the capacity limit, as modeled in (23), and in the case of activation of the upward reserve, the state-of-energy must remain non-negative, as enforced in (22). The actual change in the state-of-energy is calculated in equation (24). Thus, the state-of-energy at time period t is equal to the one at the previous time period, to which we add the energy that entered the battery storage at t , and subtract the energy that is discharged from it. Again, it is assumed that only a certain proportion of the reserved capacity is activated in both directions ($A^{\text{u}}, A^{\text{d}}$).

$$0 \leq soe_t \leq SOE^{\text{b}}, \quad \forall t \quad (21)$$

$$soe_{t-1} + (p_t^{\text{ch}} - p_t^{r, \text{ch}}) \cdot \eta^{\text{ch}} \cdot \Delta t - (p_t^{\text{dis}} + p_t^{i, \text{dis}}) \cdot \Delta t / \eta^{\text{dis}} \geq 0, \quad \forall t \quad (22)$$

$$soe_{t-1} + (p_t^{\text{ch}} + p_t^{i, \text{ch}}) \cdot \eta^{\text{ch}} \cdot \Delta t - (p_t^{\text{dis}} - p_t^{r, \text{dis}}) \cdot \Delta t / \eta^{\text{dis}} \leq SOE^{\text{b}}, \quad \forall t \quad (23)$$

$$soe_t = soe_{t-1} + (p_t^{\text{ch}} - A^{\text{u}} \cdot p_t^{r, \text{ch}} + A^{\text{d}} \cdot p_t^{i, \text{ch}}) \cdot \eta^{\text{ch}} \cdot \Delta t - (p_t^{\text{dis}} - A^{\text{d}} \cdot p_t^{r, \text{dis}} + A^{\text{u}} \cdot p_t^{i, \text{dis}}) \cdot \Delta t / \eta^{\text{dis}}, \quad \forall t \quad (24)$$

The authors in [26] present a battery storage model that was used, which considers the reduced maximum charging power at high state-of-energy of the battery storage. For all the modeling details, we kindly refer the reader to this reference due to page limit.

Finally, constraints (25)–(31) describe the operation of the electrolyzer. The electrolyzer must operate in the range between 10% of the rated power [27] and the rated power P^{el} , given by (25) and (26). As with the battery storage, the electrolyzer must also comply with these restrictions

when providing reserve. Therefore, a reduction in electricity consumption can be achieved ranging from the current consumption p_t^{el} to the minimum consumption, as modeled in (27). On the other hand, an increase in the consumption can only be achieved up to the rated power of the electrolyzer (28).

$$p_t^{\text{el}} \geq 0.1 \cdot P^{\text{el}} \cdot w_t, \quad \forall t \quad (25)$$

$$p_t^{\text{el}} \leq P^{\text{el}} \cdot w_t, \quad \forall t \quad (26)$$

$$p_t^{\text{r,el}} \leq p_t^{\text{el}} - 0.1 \cdot P^{\text{el}} \cdot w_t, \quad \forall t \quad (27)$$

$$p_t^{\text{i,el}} \leq P^{\text{el}} \cdot w_t - p_t^{\text{el}}, \quad \forall t \quad (28)$$

Equation (29) describes how much electricity $p_t^{\text{ee,el}}$ is needed to produce a certain amount of hydrogen h_t^{el} . The efficiency of the electrolyzer (η_t^{el}) depends on its operating point. At 10% of the rated power the efficiency is 80%, and at the rated power it is reduced to 70% [28]. Therefore, the mentioned equation needs to be linearized, and the result of linearization is (30). Variable $p_t^{\text{ee,el}}$ denotes the electricity that needs to be provided to the electrolyzer to produce h_t^{el} hydrogen, and that electricity in this case is equal to the sum of the energy purchased in the day-ahead market and the balancing energy (31).

$$h_t^{\text{el}} = p_t^{\text{ee,el}} \cdot \eta_t^{\text{el}}, \quad \forall t \quad (29)$$

$$h_t^{\text{el}} = 0.689 \cdot p_t^{\text{ee,el}} + 0.011 \cdot P^{\text{el}} \cdot w_t, \quad \forall t \quad (30)$$

$$h_t^{\text{el}} = 0.689 \cdot (p_t^{\text{el}} + A^{\text{d}} \cdot p_t^{\text{i,el}} - A^{\text{u}} \cdot p_t^{\text{r,el}}) + 0.011 \cdot P^{\text{el}} \cdot w_t, \quad \forall t \quad (31)$$

III. CASE STUDY

A. Input Data

We present two case studies. The first is to consider the impact of the units' size and the market prices on the facility's operation, and the second is to determine the impact of having a PV in such a plant. Prices in the electricity day-ahead market are taken from the wholesale market of the Croatian Power Exchange (CROPEX) [29], while prices from the Central European Gas Hub (CEGH) [30] are used for the gas day-ahead market, both for period 2019–2021. In the electricity system, the grid tariff is charged both for the energy and power components. The energy component has two tariffs and is charged only in case of withdrawal, while the power component is charged for both directions and is calculated as the maximum monthly average power during 15-minute periods. Prices are defined by the Croatian Transmission System Operator (HOPS) [31]. On the other hand, the gas system grid tariff charges only for the energy component, but in both directions, and is defined monthly by the Croatian Gas System Operator (Plinacro) [32].

Automatic frequency restoration reserve (aFRR) activation of 20% in both directions ($A^{\text{u}}, A^{\text{d}}$) is assumed. Reservation of the capacity is charged at 12.36 €/MW in the upward direction and 12.05 €/MW in the downward direction. These are the prices in Croatia in the year 2021 [33]. For activated balancing energy in the upward direction, the transmission system operator pays the provider 40% higher price than the

one in the day-ahead market, and for the downward direction, the provider pays the transmission system operator 40% lower price than the one in the day-ahead market [31].

Data on PV production are taken from [34] for Croatia with an installed capacity 18 MW. The rid injection limit of the plant is set to 65 MW, while the withdrawal limit is 40 MW. Three scenarios are created to assess the impact of the installed capacities of the battery storage and the electrolyzer on the facility's operation:

$$(S1) \ SOE^{\text{max}} = 7.5 \text{ MWh}, P^{\text{b}} = 7.5 \text{ MW}, P^{\text{el}} = 7.5 \text{ MW}$$

$$(S2) \ SOE^{\text{max}} = 10 \text{ MWh}, P^{\text{b}} = 10 \text{ MW}, P^{\text{el}} = 7.5 \text{ MW}$$

$$(S3) \ SOE^{\text{max}} = 7.5 \text{ MWh}, P^{\text{b}} = 7.5 \text{ MW}, P^{\text{el}} = 10 \text{ MW}$$

In all scenarios, battery charging and discharging efficiencies are set to 0.92.

B. Impact of Market Prices and Installed Capacities

Fig. 2 shows revenues (R) and costs (C) for all three scenarios in the period 2019–2021. Total profit is the highest in 2021 due to extremely high prices and price spreads in the electricity day-ahead market, and the lowest in 2020 due to the effects of the pandemic, i.e. low prices and price spreads. In 2019 and 2020, the largest share of the total profit comes from the capacity reservation (dark blue columns), more precisely about 60% in the year 2019 and about 70% in 2020, depending on the scenario. In the year 2021, its share is reduced to approximately 30% because the highest share in profit (over 50%) is generated in the electricity day-ahead market. Such high electricity day-ahead market profit is due to the aforementioned high and volatile prices — the average price on CROPEX in 2021 was 114.7 €/MWh, while in 2019 and 2020 around 40 €/MWh. This is why the share of electricity day-ahead profit in 2019 and 2020 is merely over 30% and 20%, respectively. The share of hydrogen sales revenue in the gas day-ahead market in total profit ranges between 5 and 10%, depending on the year and the scenario. The impact of the installed battery storage and electrolyzer capacities is visible in scenarios. By increasing the installed battery capacity (S2), it is possible to increase the provision of reserves from the battery storage in both directions by approximately 30% for all three years as compared to the other two scenarios, as presented in Fig. 3 (dark and light blue bars). On the other hand, the ratio of purchased and sold energy from the battery storage is constant throughout the scenarios.

In case of higher installed power of the electrolyzer (S3), the possibility of selling hydrogen increases, and therefore the annual hydrogen production, along with the revenue from the gas day-ahead market (light blue in Fig. 2), increases by the same percentage as the installed capacity. The increase in production occurs solely due to the increase in installed capacity because the electrolyzer operates the same amount of time through all scenarios. However, changes in the amount of electrolyzer operation occur over the years, as given in Fig. 4. In the years 2019 and 2020, the electrolyzer operates 92% and 96% of the year (the upper two graphs), respectively, due to relatively low prices in the electricity market. As the prices begin to rise in the year 2021 (blue curve on the last graph),

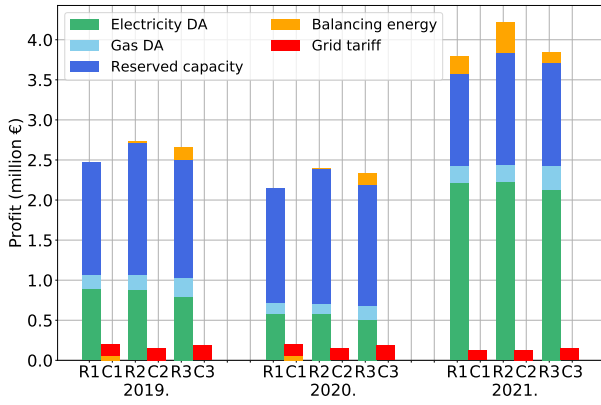


Fig. 2: Breakdown of yearly cost (C) and revenue (R) for the 2019–2021 period in all three scenarios (“R1” — revenue in S1)

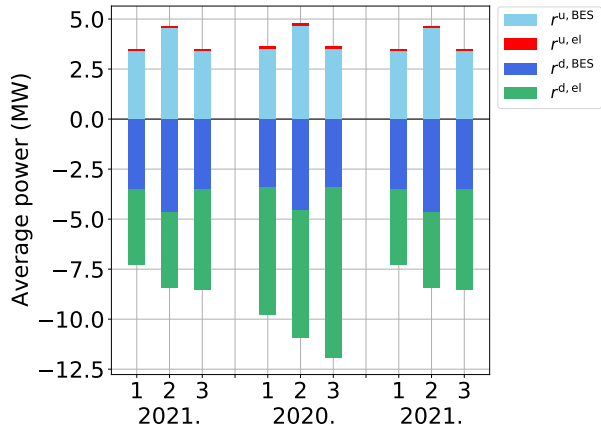


Fig. 3: Reserve provision for the period 2019–2021 and all three scenarios

the amount of time the electrolyzer operates reduces to only 57% of the year. The red curve on the last graph is mostly at 0 MW (electrolyzer is turned off) and has occasional increases to its technical minimum. In the case of 2019 and 2020, most of the time the electrolyzer operates at the technical minimum with occasional shutdowns and increases to its maximum capacity. Such changes occur to provide reserve services to the electricity system — increase operation to its maximum to be able to provide the upward reserve or operate at the technical minimum to be able to provide the downward reserve. The electrolyzer provides the highest amount of reserve in the downward direction throughout all years and all scenarios, given in Fig. 3, with the provision of reserves in both directions decreasing in 2021 due to an extremely large increase in prices.

C. Benefit of Having PV

To compare the impact of the PV on the facility’s profitability, calculations were made for all three scenarios for the year 2021, with and without PV. When the purchase and sale prices of electricity are equal in a certain time period, PV does not make a difference in the operation of such a plant. However, if grid tariffs are considered, buying electricity results in higher

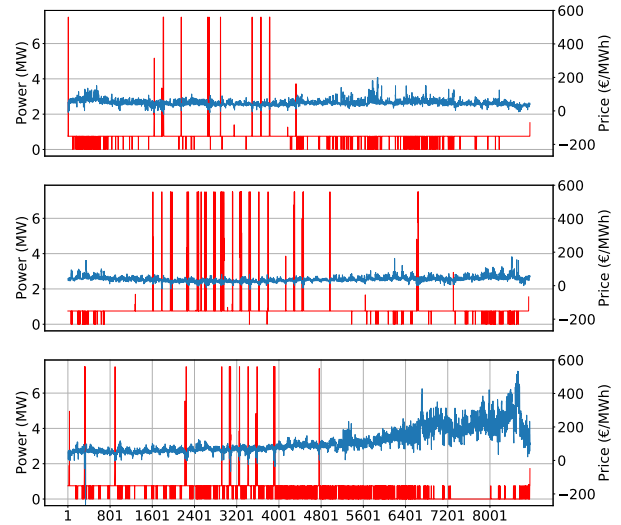


Fig. 4: Electrolyzer operation (red curve, left-hand axis) in year 2019 (top), 2020 (middle) and 2021 (bottom) vs electricity day-ahead market prices (blue curve, right-hand axis)

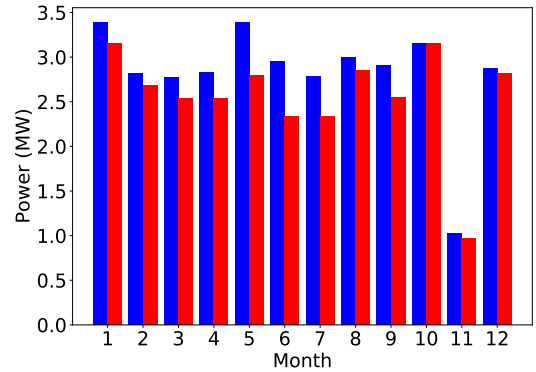


Fig. 5: The highest withdrawn power in S1 in case of installed PV (red bars) and without it (blue bars) in 2021

costs than the possible revenue that a sale would bring at the same time period. Therefore, electricity produced from PV is used for self-supply purposes and thus enables cost reduction of the facility. Fig. (5) shows the maximum withdrawn power from the network without (blue bars) and with (red bars) the PV plant for each month in S1. With available PV, peak withdrawal power is reduced in all months. The same trend is observed in the other two scenarios, as well. The small reduction in months 10–12 occurs due to high prices in the electricity market, which makes it more profitable to sell the produced energy than to use it locally to reduce the grid tariff cost. Average prices in those months were 203 €/MWh, 215 €/MWh, and 251 €/MWh, respectively. The energy component of the grid tariff is reduced with the use of PV in all three scenarios by approximately 37%. In total, the grid costs decreased by around 10%. In addition, an increase in the number of time periods in which the electrolyzer operates of around 5% can be observed, because the electricity needed for its operation does not have to be taken from the grid.

IV. CONCLUSION

This paper analyzes a facility consisting of a PV, battery storage, and an electrolyzer, and which participates in the day-ahead and reserve markets. The rise in prices in 2021 yields trading in the electricity day-ahead market as the most profitable source of income, while in the earlier years the majority of profit came from the reserve capacity. On the other hand, such high prices reduced the annual period of operation of the electrolyzer.

Changes in the capacity of the electrolyzer or battery storage do not affect their operation, they only allow a change in the range of their action, which is then reflected in the final profit. Finally, the possession of PV allows further reduction of the costs caused by the grid tariff and increased operating time of the electrolyzer. In further research, we will examine the impact fuel cell could have on the proposed framework, as well as the modeling of the hydrogen and the gas systems.

ACKNOWLEDGMENT

This work was supported by the Croatian Science Foundation and European Union through the European Social Fund under project Flexibility of Converter-based Microgrids -- FLEXIBASE (PZS-2019-02-7747).

REFERENCES

- [1] E. C. (EC), "Paris agreement." https://ec.europa.eu/clima/eu-action/international-action-climate-change/climate-negotiations/paris-agreement_en, December 2015. Accessed in January 2022.
- [2] U. S. E. P. A. (EPA), "Sources of greenhouse gas emissions." <https://www.epa.gov/ghgemissions/sources-greenhouse-gas-emissions>, July 2021. Accessed in January 2022.
- [3] E. C. (EC), "Regulation of the european parliament and of the council on the internal markets for renewable and natural gases and for hydrogen." <https://eur-lex.europa.eu/legal-content/EN/TXT/?uri=CELEX:52021PC0804>, December 2021. Accessed in January 2022.
- [4] EUDP, "Energy storage – hydrogen injected into the gas grid via electrolysis field." May 2020. Accessed in January 2022.
- [5] PwC, "Hyway 27: hydrogen transmission using the existing natural gas grid? final report for the ministry of economic affairs and climate policy," June 2021. Accessed in January 2022.
- [6] B. den Ouden, "A hydrogen exchange for the climate." <https://www.government.nl/binaries/government/documents/reports/2020/09/24/a-hydrogen-exchange-for-the-climate/A+Hydrogen+exchange+for+the+Climate.pdf>, 2020. Accessed in January 2022.
- [7] R. Sioshansi, P. Denholm, J. Arteaga, S. Awara, S. Bhattacharjee, A. Botterud, W. Cole, A. Cortés, A. d. Queiroz, J. DeCarolis, Z. Ding, N. DiOrío, Y. Dvorkin, U. Helman, J. X. Johnson, I. Konstantelos, T. Mai, H. Pandžić, D. Sodano, G. Stephen, A. Svoboda, H. Zareipour, and Z. Zhang, "Energy-storage modeling: State-of-the-art and future research directions," *IEEE Transactions on Power Systems*, vol. 37, no. 2, pp. 860–875, 2022.
- [8] F. Conte, S. Massucco, G.-P. Schiapparelli, and F. Silvestro, "Day-ahead and intra-day planning of integrated bess-pv systems providing frequency regulation," *IEEE Transactions on Sustainable Energy*, vol. 11, no. 3, pp. 1797–1806, 2020.
- [9] Z. Luburić, H. Pandžić, T. Plavšić, L. Teklić, and V. Valentić, "Role of energy storage in ensuring transmission system adequacy and security," *Energy*, vol. 156, pp. 229–239, 2018.
- [10] D. Gusain, M. Cvetković, R. Bentvlsen, and P. Palensky, "Technical assessment of large scale pem electrolyzers as flexibility service providers," in *2020 IEEE 29th International Symposium on Industrial Electronics (ISIE)*, pp. 1074–1078, 2020.
- [11] U. Mukherjee, S. Walker, A. Maroufmashat, M. Fowler, and A. Elkamel, "Power-to-gas to meet transportation demand while providing ancillary services to the electrical grid," in *2016 IEEE Smart Energy Grid Engineering (SEGE)*, pp. 221–225, 2016.
- [12] C. Peter, E. Vrettos, and F. N. Büchi, "Polymer electrolyte membrane electrolyzer and fuel cell system characterization for power system frequency control," *International Journal of Electrical Power & Energy Systems*, vol. 141, p. 108121, 2022.
- [13] S. Z. Hassan, H. Li, T. Kamal, S. Mumtaz, and L. Khan, "Fuel cell/electrolyzer/ultra-capacitor hybrid power system: Focus on integration, power control and grid synchronization," in *2016 13th International Bhurban Conference on Applied Sciences and Technology (IBCAST)*, pp. 231–237, 2016.
- [14] B. Wang, Y. Liang, J. Zheng, R. Qiu, M. Yuan, and H. Zhang, "An milp model for the reformation of natural gas pipeline networks with hydrogen injection," *International Journal of Hydrogen Energy*, vol. 43, no. 33, pp. 16141–16153, 2018.
- [15] I. Saedi, S. Mhanna, and P. Mancarella, "Integrated electricity and gas system modelling with hydrogen injections and gas composition tracking," *Applied Energy*, vol. 303, p. 117598, 2021.
- [16] L. M. Romeo, M. Cavana, M. Bailera, P. Leone, B. Peña, and P. Lisbona, "Non-stoichiometric methanation as strategy to overcome the limitations of green hydrogen injection into the natural gas grid." *Applied Energy*, vol. 309, p. 118462, 2022.
- [17] K. Stewart, L. Lair, B. De La Torre, N. L. Phan, R. Das, D. Gonzalez, R. C. Lo, and Y. Yang, "Modeling and optimization of an alkaline water electrolysis for hydrogen production," in *2021 IEEE Green Energy and Smart Systems Conference (IGESSC)*, pp. 1–6, 2021.
- [18] W. Pirom and A. Srisiriwat, "Electrical energy-based hydrogen production via pem water electrolysis for sustainable energy," in *2022 International Electrical Engineering Congress (iEECON)*, pp. 1–4, 2022.
- [19] A. Khalilnejad, A. Sundararajan, and A. Sarwat, "Performance evaluation of optimal photovoltaic-electrolyzer system with the purpose of maximum hydrogen storage," in *2016 IEEE/IAS 52nd Industrial and Commercial Power Systems Technical Conference (I CPS)*, pp. 1–9, 2016.
- [20] W. Gao, V. Zheglov, G. Wang, and S. M. Mahajan, "Pv - wind - fuel cell - electrolyzer micro-grid modeling and control in real time digital simulator," in *2009 International Conference on Clean Electrical Power*, pp. 29–34, 2009.
- [21] A. Cano, F. Jurado, H. Sánchez, M. Castañeda, and L. M. Fernández, "Sizing and energy management of a stand-alone pv/hydrogen/battery-based hybrid system," in *International Symposium on Power Electronics Power Electronics, Electrical Drives, Automation and Motion*, pp. 969–973, 2012.
- [22] A. M. Abomazid, N. El-Taweel, and H. E. Farag, "Optimal energy management of hydrogen energy facility using integrated battery energy storage and solar photovoltaic systems," *IEEE Transactions on Sustainable Energy*, pp. 1–1, 2022.
- [23] M. Castañeda, L. M. Fernández, H. Sánchez, A. Cano, and F. Jurado, "Sizing methods for stand-alone hybrid systems based on renewable energies and hydrogen," in *2012 16th IEEE Mediterranean Electrotechnical Conference*, pp. 832–835, 2012.
- [24] R. Jallouli and L. Krichen, "Sizing, techno-economic and generation management analysis of a stand alone photovoltaic power unit including storage devices," *Energy*, vol. 40, no. 1, pp. 196–209, 2012.
- [25] A. Ibáñez-Rioja, P. Puranen, L. Järvinen, A. Kosonen, V. Ruuskanen, J. Ahola, and J. Koponen, "Simulation methodology for an off-grid solar–battery–water electrolyzer plant: Simultaneous optimization of component capacities and system control," *Applied Energy*, vol. 307, p. 118157, 2022.
- [26] H. Pandžić and V. Bobanac, "An accurate charging model of battery energy storage," *IEEE Transactions on Power Systems*, vol. 34, no. 2, pp. 1416–1426, 2019.
- [27] "Global hydrogen review 2021," tech. rep., IEA, 2021.
- [28] Nel, "Containerized PEM Electrolyser — Nel Hydrogen," 2021.
- [29] "CROPEX Croatian Power Exchange." <https://www.cropex.hr/hr/trgovanja/dan-unaprijed-trziste/rezultati-dan-unaprijed-trzista.html>. Accessed in January 2022.
- [30] "CEGH." <https://www.cegh.at/>. Accessed in January 2022.
- [31] "HOPS." <https://www.hops.hr/>. Accessed in January 2022.
- [32] "Plinacro." <https://www.plinacro.hr/>. Accessed in January 2022.
- [33] "ENTSO-E Transparency Platform." <https://transparency.entsoe.eu/dashboard/show>. Accessed in January 2022.
- [34] "Renewables.ninja." www.renewables.ninja. Accessed in January 2022.